Available online at www.sciencedirect.com
SCIENCE DIRECT®
Journal of Marine Systems 45 (2004) 55–73
JOURNAL OF MARINE SYSTEMS
www.elsevier.com/locate/jmarsys

Fronts in the Southern Indian Ocean as inferred from satellite sea surface temperature data

Andrey G. Kostianoy[a,*], Anna I. Ginzburg[a], Michel Frankignoulle[b], Bruno Delille[b]

[a] P.P. Shirshov Institute of Oceanology, Russian Academy of Sciences, Moscow, Russia
[b] Unité d'Océanographie Chimique, MARE, University of Liège, Belgium

Received 4 April 2002; accepted 8 September 2003

Abstract

Sea surface temperature (SST) derived from the weekly measurements made by the Advanced Very High Resolution Radiometers (AVHRR) of NOAA satellites was used to investigate the structure and space-time variability of large-scale fronts in the Southern Indian Ocean (30–60°S and 20–150°E) during the period of 1997–1999. Monthly SST gradient maps provided an overall view of five basic fronts: the North and South Subtropical fronts (NSTF and SSTF, respectively), the Agulhas Front (AF), the Subantarctic Front (SAF), and the Polar Front (PF). Mean location of the fronts and associated SST and SST gradients with corresponding standard deviations were calculated at each 10°-spaced longitude. A double structure of the NSTF, SAF, and PF was demonstrated as well as the meandering of all fronts with amplitudes of 2–5° in latitude and wavelength of several degrees in longitude. Convergence and transient interaction between neighboring fronts appear to occur not only in the Crozet and Kerguelen regions, but in other regions as well. The mean locations and SST range of every front are in good agreement with previous work based on hydrographic surveys [J. Geophys. Res. 101 (1996) 3675], although some details are different (in particular, the larger zonal extent of the NSTF and the wider frontal SST ranges than previously observed). A good correspondence of the measurements made during two hydrographic surveys in the Kerguelen region (22 January–3 February 1999) and in the Tasmania region (3–22 March 1998) with satellite SST and SST gradient maps was found.

Keywords: Remote sensing; Sea surface temperature; Oceanic fronts; Polar fronts; Southern Ocean; Indian sector (30–60°S and 20–150°E)

1. Introduction

Investigations of large-scale circulation and related frontal features in the Southern Ocean, including the Indian sector, have begun in the 1920s to 1950s (Sarukhanian and Smirnov, 1986; Belkin and Gordon, 1996). However, most studies of the Southern Indian Ocean fronts were carried out during 1980s to 1990s (Lutjeharms, 1981; Deacon, 1982, 1983; Gambéroni et al., 1982; Edwards and Emery, 1982; Colton and Chase, 1983; Lutjeharms and Valentine, 1984; Belkin, 1989a,b; Park et al., 1991, 1993, 2001; Tomczak and Godfrey, 1994; Orsi et al., 1995; Park and Gambéroni, 1995, 1997; Rintoul et al., 1997; Neiman et al., 1997; Holliday and Read, 1998; Smythe-Wright et al., 1998; Rintoul and Bullister, 1999; Pakhomov et al., 2000; Pollard and Read, 2001; Rintoul and Sokolov, 2001;

* Corresponding author. Tel.: +7-095-124-8810; fax: +7-095-124-5983.
E-mail address: kostianoy@online.ru (A.G. Kostianoy).

0924-7963/$ - see front matter © 2003 Elsevier B.V. All rights reserved.
doi:10.1016/j.jmarsys.2003.09.004

Rintoul and Trull, 2001). A comprehensive review of all available meridional hydrographic sections across the fronts located in the region between Greenwich meridian and Tasmania together with published papers, with consideration of the criteria for determination of different fronts, has been made by Belkin and Gordon (1996). The Southern Indian Ocean was shown to feature a complicated frontal system of quasi-zonal fronts with remarkable regional differences determined by peculiarities of bottom topography (Fig. 1). Five basic fronts are recognized there: the Agulhas Front (AF) associated with the Agulhas Retroflection, the North and South Subtropical fronts (NSTF and SSTF, respectively) as the northern and southern boundaries of the Subtropical Frontal Zone, and the Subantarctic and Polar fronts (SAF and PF, respectively) as the northern and southern boundaries of the Polar Frontal Zone. Three of the latter fronts have a circumpolar character related to the jets of the Antarctic Circumpolar Current; the NSTF is supposed to have wind-driven nature (Belkin and Gordon, 1996).

Complicated frontal features arise from the merging of neighboring fronts in the regions corresponding to pronounced bottom topography peculiarities, as in the Crozet region (triple AF/SSTF/SAF front named the "Crozet Front") and in the Kerguelen Basin (AF/SSTF/SAF or AF/SSTF/SAF/PF frontal structures) (Belkin and Gordon, 1996). However, Holliday and Read (1998), according to their continuously sampled surface temperature and salinity data, supposed that these features could result from wide spacing (about 100 km usually) between hydrographic stations. Moreover, in the cases of high space-time variability of a front (for example, the "Crozet Front"), even a section made in a few days cannot be considered synoptic (Park and Gambéroni, 1997). Furthermore, the hydrographic data coverage of the Southern Indian Ocean is rather irregular, with data sparse areas in the regions west of the Crozet Plateau, east of the Ker-

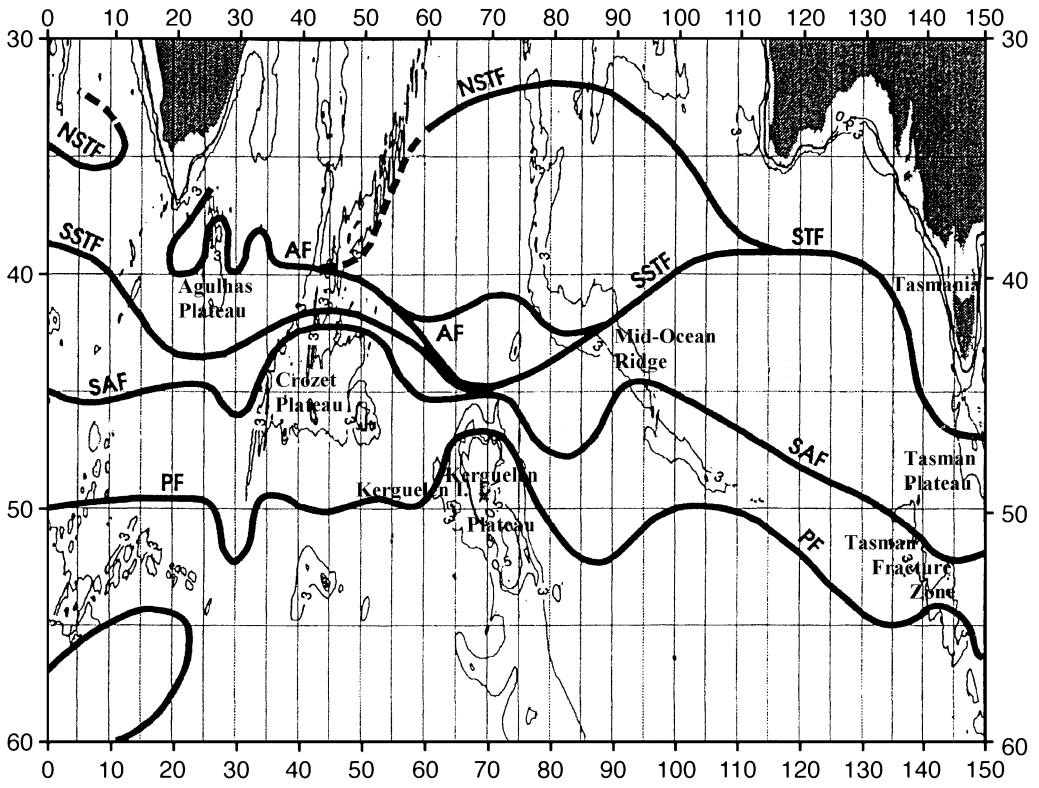

Fig. 1. Study area with frontal paths according to Belkin and Gordon (1996, Fig. 4). Notation: NSTF and SSTF—North and South Subtropical fronts, respectively; AF—the Agulhas Front; SAF—Subantarctic Front; PF—Polar Front.

guelen Plateau, and north of 37°S (Belkin and Gordon, 1996). Hence, detailed and regular synoptic surveys are needed—especially in the regions where fronts are merging and splitting—to have a comprehensive picture of the frontal structure at the basin scale.

Because all five fronts in the Southern Indian Ocean have surface temperature signatures (Belkin and Gordon, 1996), reliable satellite sea surface temperature (SST) data with high spatial and temporal resolution can be used to investigate the variability of the positions of the fronts and their intensity as well. Satellite SST maps have already been used to study dynamics of the PF (Moore et al., 1997, 1999), while Kazmin and Rienecker (1996) used satellite SST data to obtain a global picture and reveal seasonal variability of the main large-scale oceanic frontal zones.

This paper represents the first investigation of the structure and space-time variability of the complete frontal system of the Southern Indian Ocean (30°–60°S, 20°–150°E) based on satellite weekly SST data set for the period of 1997–1999, with an emphasis on poorly known or unknown aspects of location or behavior of different fronts. Furthermore, some examples of nearly synchronous field and satellite observations of fronts in the Kerguelen region (January–February 1999) and in the Tasmania region (March 1998) are considered.

2. Data and methods

The weekly mean Multichannel Sea Surface Temperature (MCSST) data of 1/6 × 1/6° (approximately

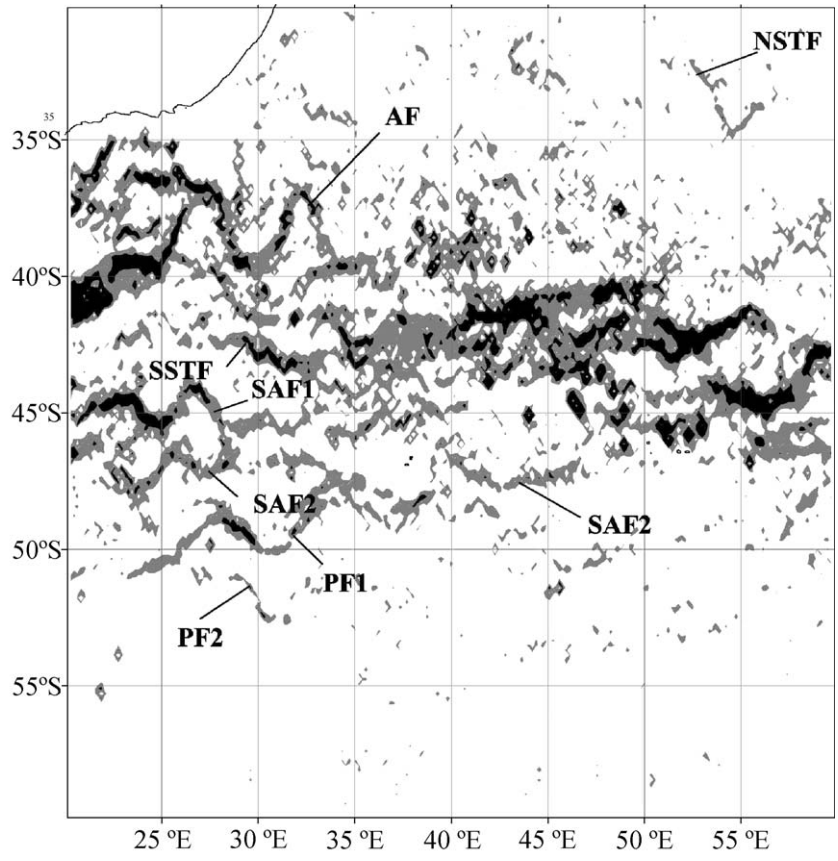

Fig. 2. Sea surface temperature (SST) gradient map for the mid-February 1997 (western region). Hereinafter (unless otherwise stated), grey tone corresponds to SST gradients of 0.02–0.04 °C/km, black tone—to SST gradients equal or higher than 0.04 °C/km.

18 km) resolution were used in this study. The SST data were derived from the Advanced Very High Resolution Radiometers (AVHRR) mounted on the satellites of the National Oceanic and Atmospheric Administration (NOAA). These data are produced in the Jet Propulsion Laboratory (JPL, USA) since 1981 with the temperature resolution of about 0.1 °C. For each grid point, the SST value is computed as the average of all MCSST measurements available for 1 week. Furthermore, JPL provides "interpolated" data sets in which the areas void of measurements (basically due to cloudiness) are filled using the Laplacian interpolation technique. For the present analysis, we used the nighttime interpolated MCSST data for the period 1997–1999 from the area between 30–60°S and 20–150°E. It should be noted that because subsurface measurements (mainly drifters data) are widely used as ground-truth data to calibrate SST values from AVHRR, the MCSST data correspond in fact to the temperature of the surface layer and can be compared with field measurements without any correction for the temperature drop in the skin layer (Fedorov and Ginsburg, 1992).

In order to retain the maximal spatial resolution of the data, the analysis was based not on the monthly averaged data, as it was made in the study of Kazmin and Rienecker (1996), but on the weekly averaged data for the weeks in the middle of each month of the 3 years. Thus, the data set used in this study comprised 36 SST maps (36 mid-month weeks) of 170 × 739 pixels. In order to obtain a picture of main fronts in the Southern Indian Ocean, the SST maps have been converted to SST gradient maps. The SST gradient was calculated for each grid point using a two-dimensional gradient operator that computes the SST difference between two adjacent points along latitude and longitude. Some examples of the SST gradient maps obtained for the western (20–60°E), central (60–100°E), and eastern (100–150°E) regions of the basin in different years are given in Figs. 2–10. In order to obtain a clear frontal pattern and to avoid "noise" in the SST gradient distribution,

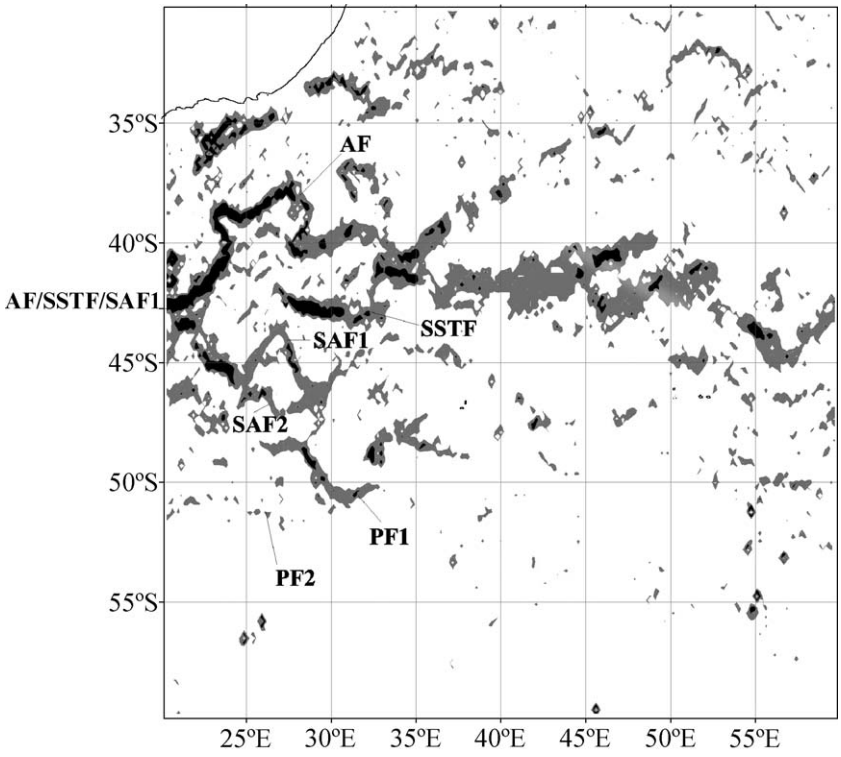

Fig. 3. Sea surface temperature gradient map for the mid-March 1997 (western region).

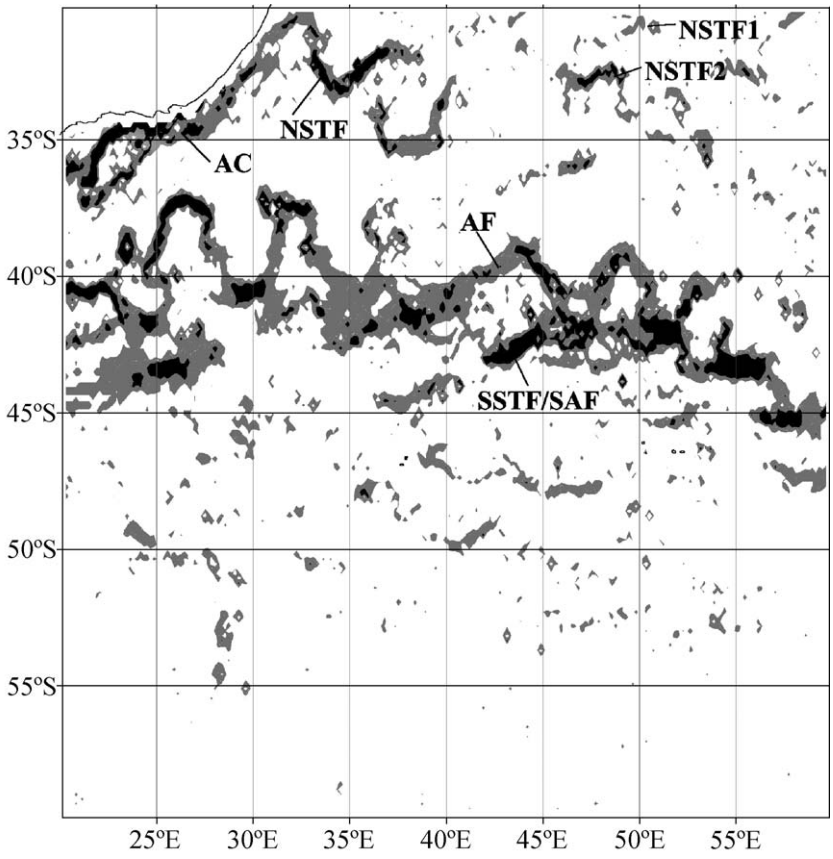

Fig. 4. Sea surface temperature gradient map for the mid-April 1998 (western region).

attention had to be paid to map only the values that were higher than 0.02 °C km^{-1}. The lowering of the threshold of the SST gradient mapping highlights the less detectable fronts south of 45°S (in the western region), but increases the "noise" of the rest of the area. However, we kept the same minimum threshold (0.02 °C km^{-1}) for all SST gradients maps of the three regions to allow the comparison of the different parts of the Southern Indian Ocean. Two gradations of shading of SST gradients were used in SST gradient maps: one in the range 0.02–0.04 °C km^{-1} and another equal or higher than 0.04 °C km^{-1}. Such kind of analysis has been already applied to the Northeast Atlantic Ocean (5–45°N) in order to detect the Azores Frontal Zone, the Northwest African upwelling front, and the Cape Verde Frontal Zone (Djenidi et al., 2000).

The digital files of the SST gradients obtained were used to determine positions of the NSTF, AF, SSTF, SAF, and PF according to the location of the appropriate maximum gradient at fixed longitudes starting from 20°E with a regular 10°-longitude interval (the interval was chosen to reduce the huge amount of data). In uncertain cases, for instance, when fronts lost their spatial coherence due to local low gradients, the appropriate SST files were used to trace the fronts. Furthermore, maps, sections, and SST characteristics of fronts presented in Belkin and Gordon (1996) were used as a reference to control the position and SST of poorly defined fronts in such cases. The same criteria were used in the cases where two or three fronts tended to merge. As a result, mean position (latitude), SST at this latter position, and SST gradient with corresponding standard deviations as well as mini-

mum and maximum values have been calculated for every front at each 10° of longitude.

Data collected during two hydrographic surveys carried out in the Southern Indian Ocean during the period under consideration were also analyzed. One of the survey was carried out during 3–22 March 1998 in the Tasmania region (about 40–55°S, 141–145°E) during the SAZ cruise (*R.S.V. Aurora Australis*) (see also (Rintoul and Trull, 2001)) and another during 22 January–3 February 1999 in the Kerguelen region (43.5–45.5°S, 61–65°E) in the course of Antares 4 cruise (*R.S.V. Marion Dufresne*). Concurrent spatial distributions of SST were obtained during both cruises, with a Sea Bird® SBE21 thermosalinograph during the SAZ cruise and with a FSI® TSG thermosalinograph during Antares 4 cruise. For both cruises, SST has been measured every minute and averaged over 5-min intervals. Thus, the distance between consecutive measurements ranged from 0.5 to 2 km depending on the ship speed.

3. Frontal pattern

3.1. Manifestation of the fronts in SST gradient maps

The set of weekly SST gradient maps for 36 mid-month weeks (for example, Figs. 2–10) gives a general indication of the structure, extent, variability, and intensity of the Southern Indian Ocean fronts. It appears obviously that the fronts in the western part of the basin (20–60°E) are marked by higher SST gradients than those situated in the central and eastern parts (Fig. 11c) where SST gradients are more diffuse and basic fronts are hardly seen in accordance to the general eastwards decrease of SST gradients generally observed in the Indian Basin (Kazmin and Rienecker, 1996). The general observed eastward decrease of frontal SST gradients can be ascribed to the decrease of overall SST latitudinal gradients across the whole investigated region (around 1.2 °C/°lat and 0.8 °C/°lat at 40°E and 140°E, respectively; Fig. 11). The AF and SSTF (37–44°S) are the best-defined fronts in the western region (Figs. 2–6 and 11) due to their high intensity (Fig. 11c), while as the intensity of frontal features decreases northward and southward, the NSTF (30–35°S), SAF (44–46°S), and PF (49–52°S) are progressively less distinguishable. In the central region (60–100°E), the most pronounced frontal system is located north of the Kerguelen Plateau, where the AF, SSTF, SAF, and PF usually merge, and southeast of the Plateau, where high SST gradients are associated with the PF (Figs. 7, 8, and 11). In the eastern region (100–150°E), some increases of SST gradients can be observed between 45°S and 55°S and are related to the SAF and PF, while between 35°S and 40°S and also south of Tasmania, some relatively marked SST gradients are associated with the NSTF and SSTF (Figs. 9–11). The northernmost front located just south of Australia, with marked seaward offshoots at about 124°E, is likely to correspond to the Leeuwin Current (Legeckis and Cresswell, 1981; Griffiths and Pearce, 1985). Basic statistics shows that in average, the strongest fronts are the AF with SST gradient of 0.037 ± 0.013 °C km^{-1} and the SSTF with SST gradient of 0.035 ± 0.013 °C km^{-1}. SST gradient was 0.030 ± 0.003 °C km^{-1} for the SAF, 0.027 ± 0.003 °C km^{-1} for the NSTF, and 0.025 ± 0.005 °C km^{-1} for the PF which appears to be the least "intense" front. Furthermore, the less intense fronts (NSTF, SAF, and PF) exhibit weak changes of the magnitude of SST gradients.

3.2. Overall frontal patterns

Fig. 11a presents the mean positions of the fronts together with the associated standard deviations at every 10° of longitude that represent both seasonal variability of the fronts location and their meandering (unfortunately, because of the meridional shifts of the fronts, their clear seasonal changes cannot be defined). The overall patterns correspond to the frontal structures presented by Belkin and Gordon (1996) (Fig. 1). In first instance, the merging of the AF, SSTF, and SAF between 50°E and 60°E which gives rise to the Crozet Frontal Zone—which is justified by the crossing of the standard deviation bars at 60°E—and the proximity of the SSTF, SAF, and PF at 70°E (the Kerguelen Frontal Zone) appear obviously in Fig. 11a. However, the frequently observed southern location of the AF when AF and SSTF/SAF are practically merged is not shown here. Furthermore, the proximity of boundaries of standard deviation ranges in the region between 20°E and 40°E could indicate a

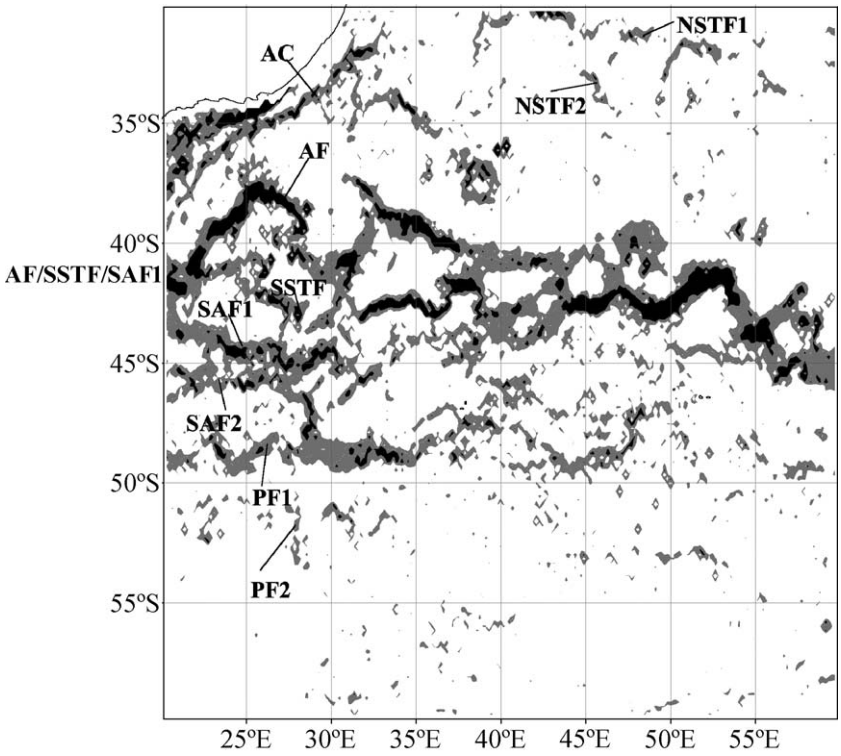

Fig. 5. Sea surface temperature gradient map for the mid-June 1999 (western region).

possible transient interaction of the AF, SSTF, and SAF there (see Section 3.3). Moreover, the poleward meanders of the SAF and PF east of the Kerguelen Plateau (90°E), the slight decrease of the distance between the SAF and PF at about 110°E after the crossing by the SAF of the Southeast Indian Ridge (Fig. 11a), as well as the location of the PF north of Kerguelen archipelago are some characteristics which can be found in the frontal patterns proposed by Belkin and Gordon (1996) (Fig. 1). This northern position of the PF is in agreement with previous studies (Fig. 102 in Sarukhanian and Smirnov, 1986; Park et al., 1991). However, some weekly maps show the PF to split in two branches rounding the Kerguelen archipelago northward and southward as it was mentioned by Belkin and Gordon (1996), and finally, the front was also observed sometimes south of the archipelago (Park and Gambéroni, 1997; Moore et al., 1999).

The satellite data analysis presents, however, some differences with regard to the work of Belkin and Gordon (1996). Both the quasi-stationary AF meanders located at 26–27°E and at 32–33°E (Grundlingh, 1978; Lutjeharms, 1981; Lutjeharms and van Ballegooyen, 1984, 1988), which appear obviously in Figs. 2–6, are not represented in Fig. 11a because they are located between the 10°-spaced longitudes chosen for the analysis. Poleward meanders of the SAF and PF at 30°E are also absent in Fig. 11a since though these meanders appear in some SST gradient maps (e.g., in Figs. 2 and 3), this is not a statistically significant and persistent feature. The extent of the NSTF in Fig. 11a is noticeably larger than previously found by Belkin and Gordon (1996) (Fig. 1) since the authors assessed that the front diverged from the AF east of about 45°E to coalesce with the SSTF at about 115°E. In Fig. 11a, the NSTF is shown from 40°E and far away from the AF. Typically, the part of the front west of 40°E is unclear due to the low SST gradients observed. However, sometimes, frontal features with enhanced SST gradients can be traced in the latitude range 30–35°S farther westward, where

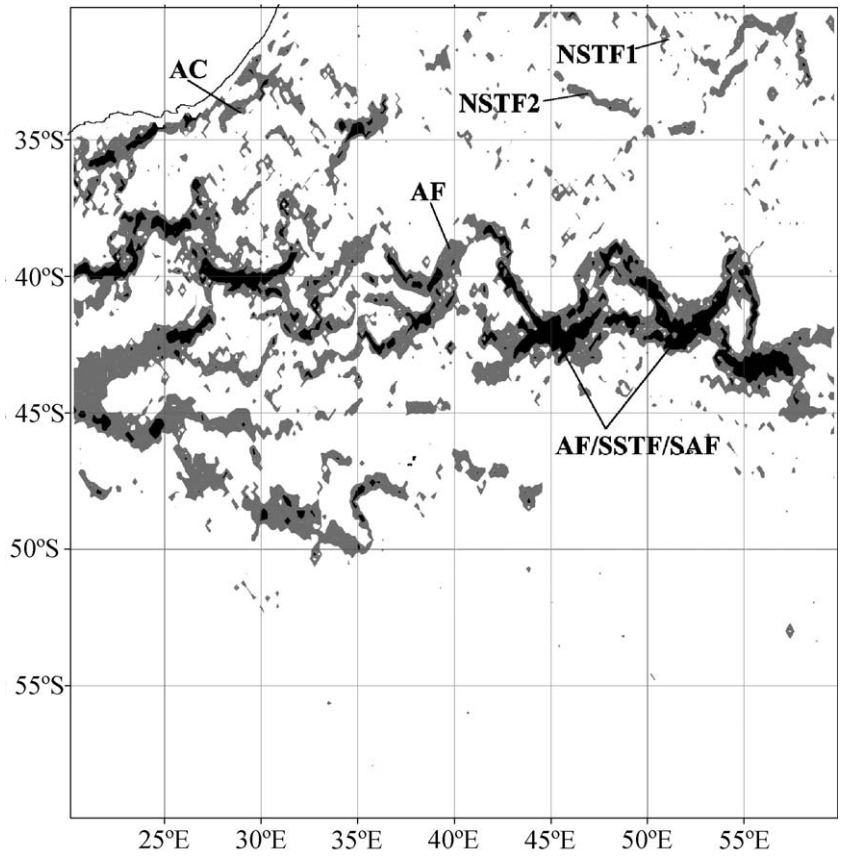

Fig. 6. Sea surface temperature gradient map for the mid-November 1998 (western region).

they reach the Agulhas Current (AC) rounding the coast of Africa. In most cases, the merging of the fronts with the AC occurs at about 30–33°E (Figs. 4–6). It is not excluded that in some cases, the westernmost part of such features in the vicinity of the AC (e.g., eddy-like structure centered at 31.5°S and 32°E in Fig. 4) is associated with a meander of the current, the so-called Natal Pulse (Lutjeharms and Roberts, 1988). However, in the general case, the frontal features within 30–35°E aligned in the seemingly zonal direction might be the westward extent of the NSTF. The question on the nature of these features has to be investigated in the future; however, in this study, they are designated as NSTF (Figs. 4–6). In the eastern region, the NSTF and SSTF are traced as different frontal structures up to about 140°E, although the close proximity and the crossing of standard deviation bars of both fronts between 110°E and 140°E could indicate a transient merging. Furthermore, the fronts probably coalesce east of 140°E to form the subtropical front (STF). Finally, the seasonal shift of the NSTF up to 5° latitude, which could be expected in accordance with the corresponding seasonal shift of the wind convergence between westerlies and easterlies (Belkin and Gordon, 1996), was not observed.

Standard deviations of the frontal zones position were made possible to compare the degree of variability between all frontal zones at each longitude (Fig. 11a). Remarkable difference in the variability is seen between longitudes 20–30°E, where the frontal zones are more stable (0.8–1.4°lat.), and the rest of the region, where they exhibit larger northward and southward displacements (1.0–2.5°lat.). Between 20°E and 60°E, the PF is constrained northward by the Crozet Plateau and southward by the Ob-Lena

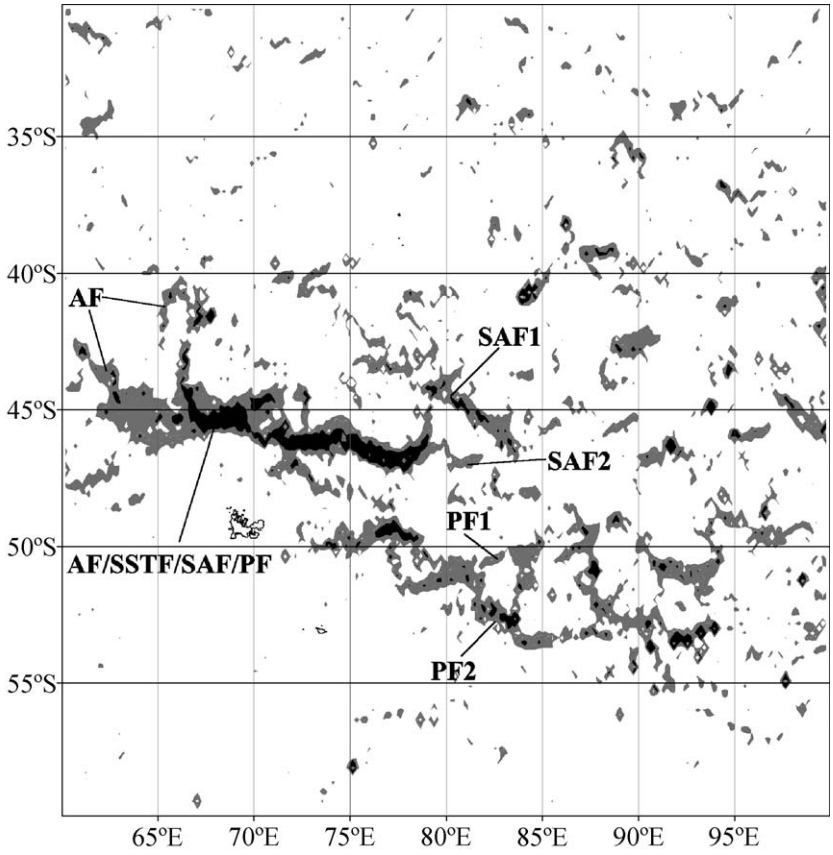

Fig. 7. Sea surface temperature gradient map for the mid-April 1997 (central region).

Rise, and thereafter exhibit a weak standard deviation. At 50°E and 60°E, since the PF is not constrained southward, the PF exhibits large latitudinal variation. As PF rounds the Kerguelen Plateau, it is constrained northward by the merging SAF/SSTF and southward by the Kerguelen archipelago so that the magnitude of latitudinal change decreases to reach a minimum at 80°E (Fig. 11a). Between 90°E and 140°E, as the PF is not constrained by peculiar bottom topography, its latitudinal movements increase. The same behaviour is observed for the SSTF which shows weak latitudinal change as it is constrained by Crozet Plateau and the AF between 40°E and 50°E or as it passes between the Kerguelen and Amsterdam plateaus (70–80°E), while its latitudinal change increases in the eastern region highlighting the role of bottom topography constraints on the latitudinal variations of the fronts positions.

3.3. Fine spatial structure of frontal zones

The weekly SST gradient maps reveal an intense spatial and temporal variability of the fronts position and configuration. All the fronts meander with a wavelength of about 3–5° in longitude and amplitude of about 2–4° in latitude. In addition to the two quasi-stationary meanders of the AF over the Agulhas Plateau (26–27°E) and at 32–33°E (Grundlingh, 1978; Lutjeharms and van Ballegooyen, 1984, 1988; Belkin and Gordon, 1996), four cyclonic meanders of the front can be episodically observed between 35°E and 55°E, where the AF crosses the Southwest Indian Ridge (Fig. 11a). Such meanders located at about 37°E, 42–44°E, 48–49°E, and 54–55°E are observed in Figs. 4 and 6. In addition, two more meanders of the AF can be formed at about 62°E and 66°E, west of the Kerguelen Plateau (Fig. 7).

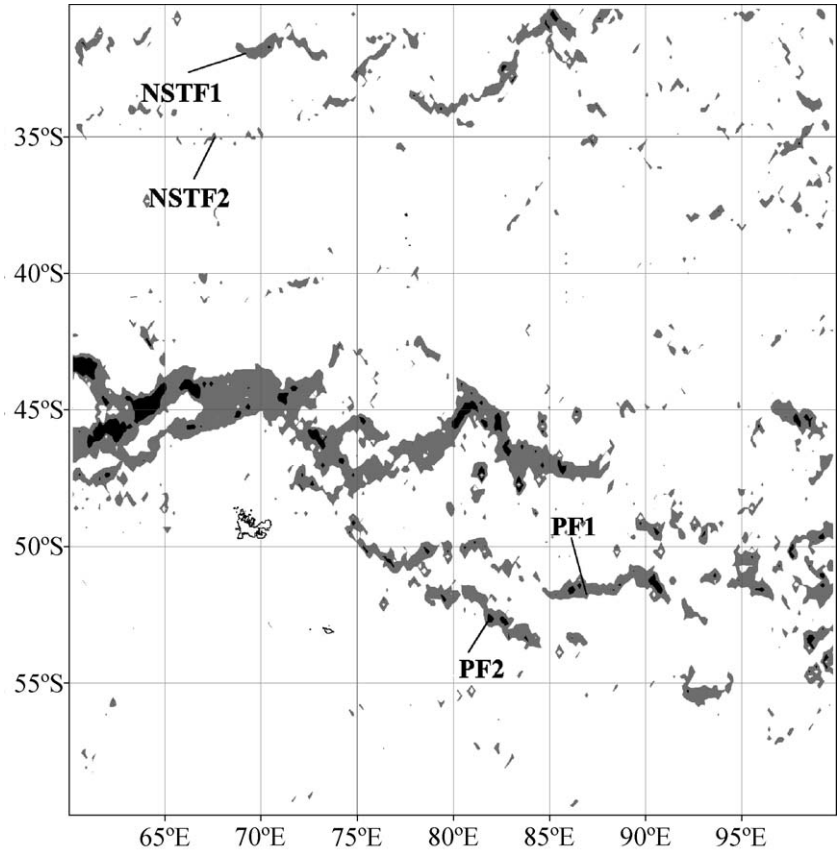

Fig. 8. Sea surface temperature gradient map for the mid-July 1997 (central region).

Hence, the Agulhas Return Current meanders from 25°E to about 66°E. It should be mentioned that similar northward excursions of the current could be expected from the trajectory of a drifting buoy in the region presented by Grundlingh (1978).

It follows from Figs. 2–6 that the amplitudes, the shapes, and the locations of the AF meanders are variable. If we compare Figs. 2 and 3, the variability timescale seems to be less than 1 month. The maximum amplitude of the meanders is about 3–4° in latitude, and wavelength is about 5–7° in longitude. Numerous patches of the increased SST gradients with diameters about 100 km or less as well as marked rings of around 200–300 km in diameter arise from the separation of the meanders from the Agulhas Return Current and are observed north of the AF in the SST gradient maps. One of such rings centered at 37.5°S and 39°E is well distinguished in Fig. 5. Similar rings were observed in the region from about 36°S to 40°S and from 25°E to 56°E in all seasons during the 3 years considered.

Because of the meandering of the fronts, the "instant" distance between neighboring fronts in the western part of the Southern Indian Ocean might be very different than the average presented in Fig. 11a. For example, southward displacement of the AF at 20°E can result in a situation where three fronts (the AF, SSTF, and SAF) are close (Figs. 3 and 5). A similar complicated frontal system can be formed at 35°E and 30°E (the AF/SSTF in Figs. 3 and 5, respectively). In the Crozet Basin (35–60°E), the AF, SSTF, and SAF can episodically converge (at 47°E in Fig. 5, at 45°E and 52°E in Fig. 6). But in other cases, especially in an area corresponding to an AF cyclonic meander, the distance between the AF and SSTF/SAF can increase up to 3° in

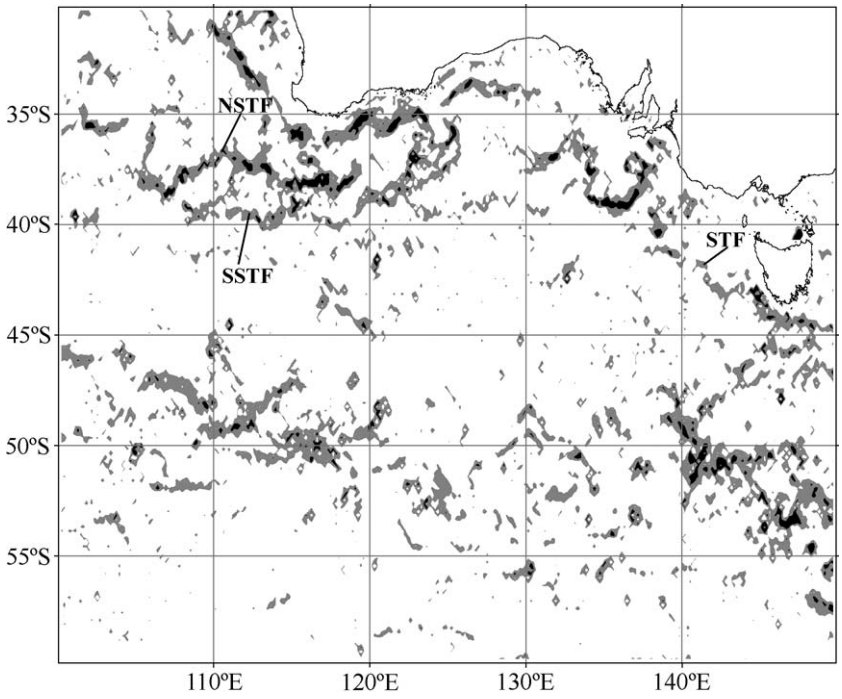

Fig. 9. Sea surface temperature gradient map for the mid-July 1999 (eastern region).

latitude (at 43°E in Fig. 4). It is evident that the dynamics of the Crozet Frontal Zone changes over time. Similarly, within the Kerguelen Frontal Zone (65–70°E), where the AF, SSTF, and SAF practically merge (Figs. 7 and 8), the distance between the AF and the SSTF/SAF can increase up to 3–4° in latitude due to the meandering of the AF (Fig. 7).

Analysis of the SST gradient maps reveals a double structure of most fronts in the basin. Some maps in the western (Figs. 4–6) and central (Fig. 8) regions imply that not one, but two meandering NSTFs (NSTF1 and NSTF2) can exist within 30–36°S at different latitudes. A bimodal path of the SAF in the western sector can also be seen in (Figs. 2, 3, and 5). In addition to the front located at about 45°S (SAF1) that is shown as the SAF in Fig. 11a, one can see another front 1–2° south of the SAF1 and north of the PF1. In Fig. 2, such a front can be distinguished from 20°E to about 50°E, and in Fig. 5 from 20°E to about 33°E. In absence of in situ measurements—in particular vertical temperature/salinity distribution—we tried to define the "belonging" of the front to the SAF or PF by its SST value. The SST value of the front in Fig. 2 at 25°E and 47°S was 7.7 °C, with SAF1 and PF1 SST values of 12.1 and 5 °C, respectively, at the same longitude and at latitudes of 45.3° and about 50°S, respectively. At 36.5°E and 48.1°S, the SST of the front was about 7.9 °C, with the PF1 SST of 6.6 °C at about 49°S. In Fig. 5, the SST of the three fronts at 25°E were 10.4 °C at 44.6°S (SAF1), 8.1 °C at 45.8°S (the front to be defined), and 3.8 °C at 49.1°S (PF1). Although SST values of 7.9–8.1 °C can also characterize the PF when it is close to the SAF (see Section 4), the confluence of the front to be defined with the SAF1 east of 50°E in Fig. 2 or at about 33°E in Fig. 5 as well as the presence of two branches of the PF south of 48°S (PF1 and PF2 in Figs. 2 and 5) allow to relate the front to the SAF (SAF2).

The SAF is known to have a bimodal path which begins at about 30°E where it turns northward or southward of the steep ridge which extends along 30–31°E (Moore et al., 1999). However, we observed both SAF1 and SAF2 between 30°E and 40°E simul-

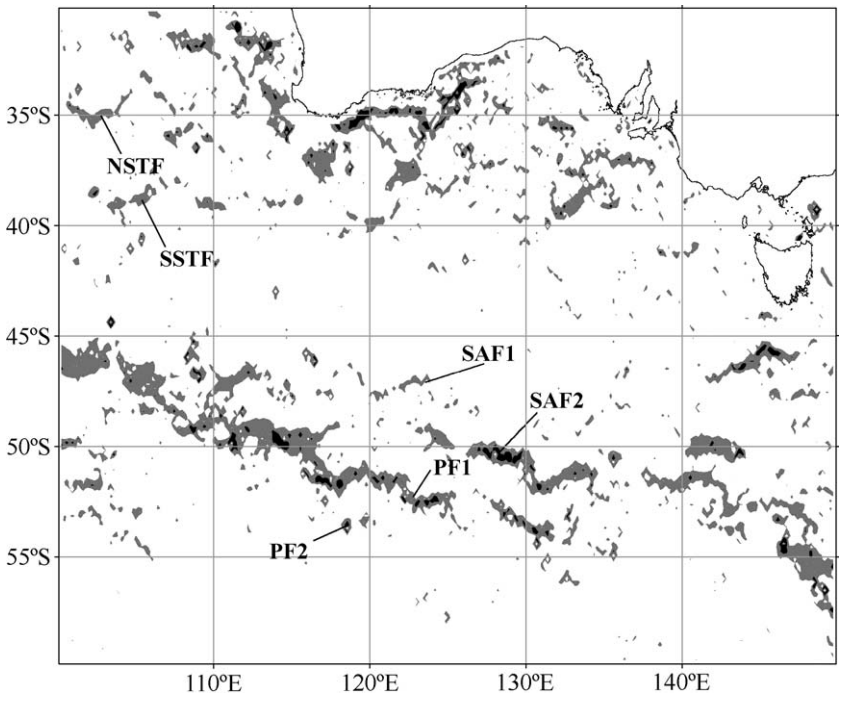

Fig. 10. Sea surface temperature gradient map for the mid-August 1998 (eastern region).

taneously (Fig. 2). The maximum separation between the fronts is observed at about 37.5°E, one front being located north of the Prince Edward Islands and another south of them. A marked northward meander of the SAF2 can be seen at about 39°E. The front rounds the Crozet Plateau from the south (a similar episodic behavior of the SAF has been mentioned by Moore et al., (1999)). At two locations (at about 47.5°S and 34°E, and 48.5°S and 38°E), the SAF2 is in the vicinity of the meandering PF1. Similar patterns of the SAF and PF have also been observed at about 35–36°E (Pakhomov et al., 2000; Pollard and Read, 2001) and between 30°E and 34°E (Read and Pollard, 1993; Belkin and Gordon, 1996; Holliday and Read, 1998). Besides, the close look at the section along 30°E in Fig. 7 of the work of Belkin and Gordon (1996) reveals two branches of the SAF, one at about 44–45°S and another one at 48.5–49°S which merges with the PF. Thus, the simultaneous existence of two subantarctic fronts and the interaction of the SAF and PF east of 30°E influenced by bottom topography appear to be repeatedly observed (see also Park et al., 2001).

Moreover, the double structure of the SAF between 20°E and 30°E appears obviously in (Figs. 2, 3, and 5). Since the phase difference between the meanders of SAF1 and SAF2 reaches 180° between 25°E and 28°E, the distance between the fronts ranges from a rather small distance at 25°E to about 3° in latitude at 27°E (Figs. 2 and 3). This double frontal structure persists for 1 month. In other cases, the southward meander of the SAF2 merges with the PF, as it occurred at 28°E in Fig. 5.

In the same way, the PF appears to have also a bimodal structure in the western part of the basin, with mean locations situated at about 49–50°S and 52°S (Figs. 2 and 5). In Fig. 2, both PF1 and PF2 have poleward meanders at about 30°E. East of the Kerguelen Plateau, at least between 75°E and 95°E, the PF has also a double structure that is well marked in Figs. 7 and 8 (PF1 and PF2 with mean positions at about 50–51°S and 53–54°S). Some SST gradient maps suggest that two branches of the SAF might exist there (for example, SAF1 and SAF2 at 79–85°E in Fig. 7). The double SAF also appears

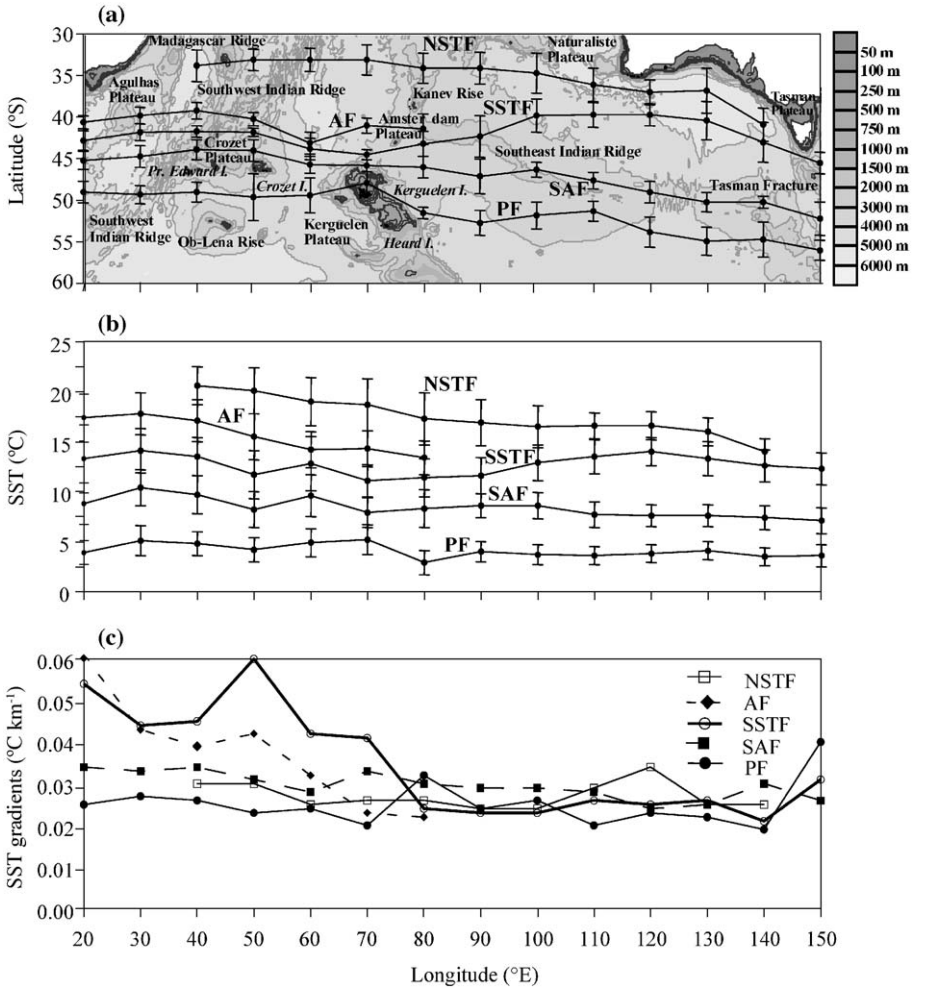

Fig. 11. (a) Bathymetry of the Southern Indian Ocean with average positions and standard deviations of the fronts, (b) average sea surface temperature (SST) and standard deviations and (c) SST gradients of the North and South Subtropical fronts (NSTF and SSTF), the Agulhas Front (AF), Subantarctic Front (SAF); and Polar Front (PF) in the Southern Indian Ocean as inferred from Multichannel SST data (1997–1999).

in the eastern part of the Southern Indian Ocean at 120–143°E in Fig. 10. It was already observed by Belkin and Gordon (1996) and its pattern is detailed in Section 3.4. Furthermore, considering the SST gradient pattern in Fig. 10, we feel that a double structure of the PF in the eastern region could exist as it has been repeatedly observed by Rintoul and Sokolov (2001) with branches at 53–54°S and 59°S. Finally, some SST maps imply that the SSTF can also have a bimodal path in the western part of the basin (for example, between 25°E and 35°E in Fig. 2).

3.4. Near-synchronous hydrographic and satellite observations of fronts in the Crozet Basin and Tasmania region

Two hydrographic surveys (SAZ and Antares 4 cruises) allow us to compare the results of field measurements near Tasmania (3–22 March 1998) and in the Crozet Basin (22 January–3 February 1999) (Dehairs et al., 2001) with near-concurrent SST gradient maps for the period of mid-February 1999 and mid-March 1998 (Figs. 12 and 13, respectively).

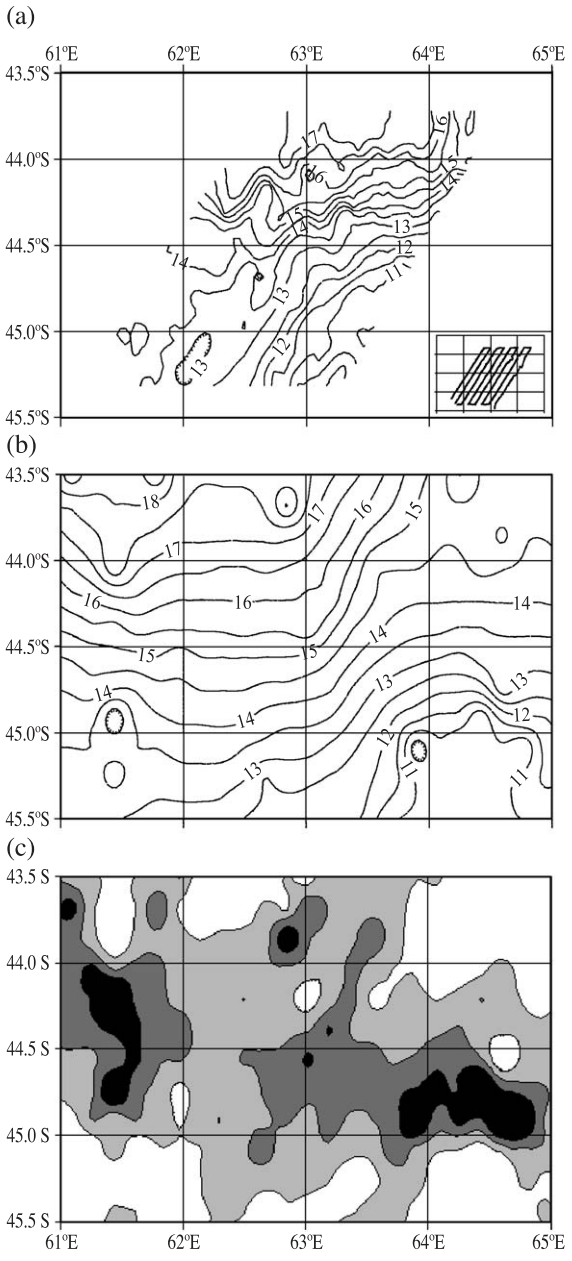

Fig. 12. Fronts in the Kerguelen region in the austral summer of 1999: (a) sea surface temperature (SST) field from hydrographic survey during 22 January–3 February 1999 (*R.S.V. Marion Dufresne*) (the ship route is shown in the insert map); (b) satellite SST map for the region of field measurements in the mid-February 1999; (c) corresponding satellite SST gradient map (light grey, dark grey, and black tones correspond to SST gradients of 0.02–0.03, 0.03–0.04, and higher than 0.04 °C/km, respectively).

The Crozet Basin hydrographic survey with high spatial resolution (about 1–2 km) revealed a frontal zone in the Kerguelen region comprising three closely spaced fronts (Fig. 12a): the SAF, SSTF, and AF. Sea surface temperature ranged from 10.5 to 12.5 °C for the SAF, from 13.5 to 15 °C for the SSTF, and from 15 to 17 °C for the AF. The frontal SST gradients in most part of the area in Fig. 12a were higher than 0.02 °C per km, i.e. exceeding the established criterion for displaying the fronts in satellite SST gradient maps. However, the distance between boundaries of the fronts in Fig. 12a is less than the resolution of the used satellite SST data (18 km). A correlation between the SST maps for the middle January (not shown here) and the mid-February (Fig. 12b) reveals an intense frontal dynamics during the period associated with the arrival of warm water from the northwest and cold water from the southeast. This leads to a further decrease of the distance between the fronts. Hence, the fronts are seen in Fig. 12c as a single frontal feature.

In the Tasmania region, three fronts can be seen in Fig. 13a: the PF (SST range of 4–5 °C), SAF (5–10 °C), and STF (11–13 °C). The SAF has a double structure at 141–142°E: the southern front (SSAF) is located at about 52°S (SST range of 6–8.5 °C) and the northern one (NSAF) at 48.5°S (9.5–11 °C). Slightly eastward (at 144°E), both branches of the SAF coalesce to form a single front with a sharp temperature change from 7.5 to 11 °C.

Satellite SST and SST gradient maps (Fig. 13b and c, respectively) display all the frontal features seen in Fig. 13a (because of the low SST gradients encountered in most part of the area, we decreased the minimum threshold for SST gradients mapping to 0.12 °C km^{-1} in Fig. 13c). In addition, satellite maps exhibit some complicated frontal features beyond the field measurements area. East of 146°E, the SAF separates again in two fronts, with a distance between them up to 3° in latitude. The SSAF merges with the PF, whereas the NSAF converges towards the southward meander of the STF. This close approach of the SAF and PF in the region situated at about 52°S in the austral summer was episodically observed by Rintoul et al. (1997). It appears that the STF structure is also variable: two branches of the front (11–11.5 °C and 12–13 °C) are observed at 142.5°E, then they coalesce at 145°E and separate again east of about 148°E. Furthermore, another frontal feature charac-

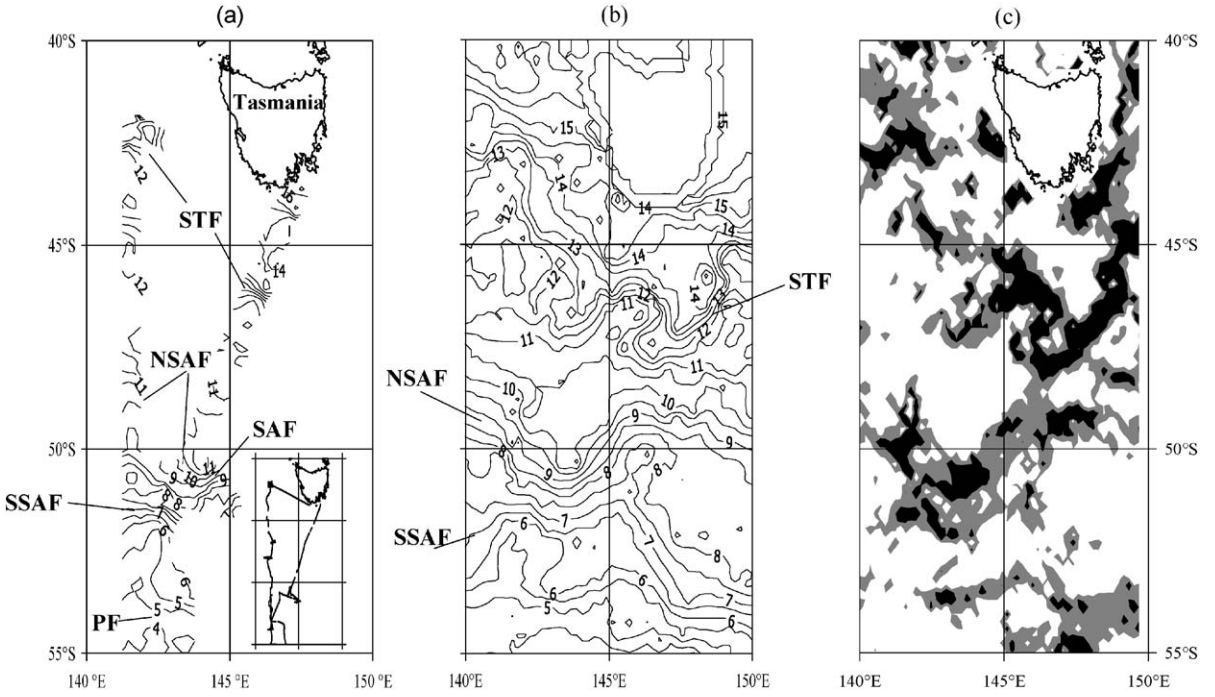

Fig. 13. Fronts in the Tasmania region in the austral summer of 1998: (a) sea surface temperature (SST) field from CTD survey during 3–22 March 1998 (*R.S.V. Aurora Australis*) (the ship route is shown in the insert map); (b) satellite SST map for the region of field measurements in the mid-March 1999; (c) corresponding satellite SST gradient map (grey tone corresponds to SST gradients of 0.012–0.02 °C/km; black tone—to higher gradients).

terized by a temperature change from 14 to 16 °C can be observed north of the STF. This additional frontal structure merges with the STF at about 142°E, 146°E, and 149°E. One can notice that the best-developed meander of the STF and subsequent convergence towards the NSAF were observed over the Tasmania Plateau. The southward meander of the NSAF and its confluence with the northward meander of the SSAF at about 143°E occurred in the vicinity of the Tasman Fracture Zone (Fig. 11a). The meanders of the NSAF and SSAF appear obviously in a sea surface height map based on TOPEX/Poseidon data for the mid-March 1998, whereas the STF with a weak density signature is not manifested in the map (Rintoul and Trull, 2001, Fig. 2).

The cyclonic eddy-like structure or meander which is observed between the two SAF branches at about 50°S and 146°E in Fig. 13c is also seen in a sea surface height map for the mid-March 1998 (Rintoul and Trull, 2001, Fig. 2). Interestingly, the similar cold-core cyclonic eddy or meander was repeatedly found on XBT sections at about the same location throughout the 1993–1994 austral summer by Rintoul et al. (1997). This implies a correlation between the feature and the bottom topography. Our analysis of SST maps for the period 1997–1999 has shown that a clear correlation between surface manifestation of the bottom-controlled meander (eddy) and season is absent. The feature was observed in May–September and December 1997, in March and October–November 1998, and in February–July and September–November 1999.

The examples considered above suggest that the available satellite SST data supply reliable information on the structure of frontal zones, their dynamics, and absolute values of the surface layer temperature.

4. SST ranges of the fronts in the Southern Indian Ocean (20–150°E)

Fig. 11b gives an indication of the variation of SST along the fronts. The temperature changes for the PF,

SAF, and SSTF are small. Minimum mean value of the PF SST at 80°E may be associated with the southward meander of the front at this longitude (Fig. 11a). It is possible that the minimum mean SST values of the SAF and SSTF observed at 50°E and 70°E (the regions of the Crozet and Kerguelen Plateaus, respectively) are due to the close approach and interaction of several fronts in these regions (Fig. 11a). The overall decrease of the mean SST of both AF and NSTF eastwards may be attributed to their moving away from the Agulhas Current that is the origin of warm water. The standard deviation of the mean SST of each front at each longitude is conditioned by both their seasonal variations and north–south displacement resulting from their meandering or interaction with neighboring fronts (Fig. 11a,b). Standard deviations of the frontal zones SST show that their SST is much variable (1.0–3.5 °C) in the western region (where frontal zones are more stable in term of position) in comparison with their SST (1.0–1.5 °C) in the eastern region (where frontal zones are more variable). Generally, the amplitude of the SST standard deviation is larger at the NSTF and is lower at the PF.

Mean SST and latitude ranges of each front in the Southern Indian Ocean are presented in Fig. 14. The SST ranges for the whole basin as well as for its

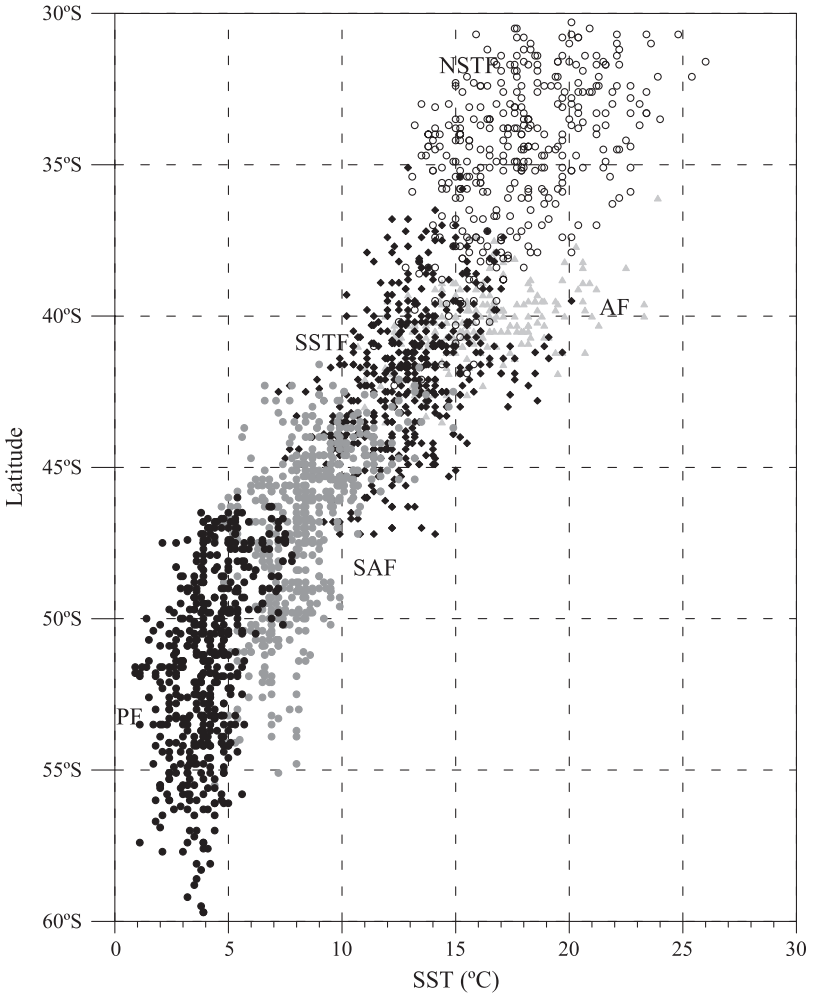

Fig. 14. Latitude-frontal sea surface temperature diagram in the Southern Indian Ocean based on satellite multichannel sea surface temperature data (1997–1999).

western (20–60°E), central (60–100°E), and eastern (100–150°E) parts are detailed in Table 1. For comparison purposes, the SST ranges for every front inferred from hydrographic sections and tables from Belkin and Gordon (1996) are given in Table 1 as well (the right-hand column). When a double structure of the fronts is encountered, SST of both fronts are taken into consideration in the corresponding SST ranges based on in situ measurements.

SST ranges as well as their boundary values obtained by two methods differ to some extent, the lowest differences being for the SAF and PF and largest for the NSTF, AF, and SSTF. On one hand, the difference can be accounted for by objective factors like interannual and seasonal temperature variability, north–south displacement of the fronts, and their interactions. For instance, the minimum SST values of the AF (10.7 °C) and SSTF (7.2 °C) correspond to September 1999 at 50°E, where the merging of the AF, SSTF, and SAF was observed at that time. The unusually wide range of the PF is associated with the frequently observed double structure of the front, when one front with surface temperature of about 3–5 °C is typically located at 50–52°S and another one either northward (6–9 °C at 46–48°S and 45°E in Fig. 9 in Belkin and Gordon, 1996) or southward (e.g., frontal surfacing isotherms 1.5–3 °C at about 59°S and 150°E in Fig. 19 in the same paper). In addition, different methods were used to determine SST ranges from satellite and field data: in the former case, the SST value at the point of maximum SST gradient was taken as a frontal SST, whereas in the latter case, both low and high boundary isotherms of a front were considered. Discrepancy may rise from the fact that in situ CTD measurements do not cover homogeneously all the regions of the Southern Indian Ocean, all the seasons at the same time, and usually have worse spatial resolution. On the other hand, a subjective factor can influence the boundary values of the frontal SST ranges based on satellite data. For example, in the cases of double structure of the SAF, it is impossible to distinguish the SAF from the PF on the base of satellite data alone. However, in most cases, the SST ranges of fronts determined from satellite data are in good agreement with those based on in situ measurements.

5. Concluding remarks

This study has demonstrated the efficiency and consistency of the analysis of satellite SST data in an investigation of the structure and both spatial and temporal variability of the position, intensity, and temperature ranges of the main fronts of the Southern Indian Ocean. The main advantage of this method is related to the use of regular SST data set with a relatively high resolution (1/6 of degree) and relatively high frequency (1 week), which provides the pattern of all fronts and frontal zones over the whole basin simultaneously.

To our best knowledge, for the first time, all five fronts have been mapped in the Southern Indian Ocean during 3 years (1997–1999) from a regular set of weekly satellite SST data, and for the first time, the intensity of each front in terms of SST gradients was calculated and compared for different regions. In general, the overall diagram of mean locations of the fronts corresponds to the structures previously observed through hydrographic data, but some details have been found to be different. In particular, the double structure of the NSTF, SAF, and PF in the

Table 1
Sea surface temperature ranges (SST) of fronts in the Southern Indian Ocean (20–150°E) inferred from satellite multichannel SST data (present study) and hydrographic in situ data by Belkin and Gordon (1996)

Fronts	SST ranges (°C)				
	Multichannel SST (present study)				In situ data (Belkin and Gordon, 1996)
	20–60°E	60–100°E	100–150°E	Total	
NSTF	14.6–26.0	13.1–24.8	11.4–22.1	11.4–26.0	16.0–23.0
AF	10.7–23.9	11–19.5	–	10.7–23.9	12.0–21.7
SSTF	7.2–20.1	7.7–18.6	9.2–17.1	7.2–20.1	9.0–17.0
SAF	4.8–14.9	4.4–13.5	4.8–11.4	4.4–14.9	5.0–14.0
PF	1.2–7.8	0.9–7.8	1.1–6.2	0.9–7.8	1.5–9.0

western, central, and eastern sectors of the Southern Indian Ocean was pointed out as well as the meandering of all fronts with amplitudes of 2–5° in latitude and wavelength of several degrees in longitude. Note that the conclusion about wavelike oscillations of the Antarctic Circumpolar Current jets, with wavelength up to 400 km, have been pointed out by Kort (1981) using the analysis of drifters trajectories. Furthermore, the variability of the fronts location and related SST values due to the meandering of the fronts, their splitting into two branches, or their merging into a single structure appears to exceed the seasonal variability of the frontal position and SST. At large scale, overall frontal position and their latitudinal changes appear to be strongly constrained by bottom topography.

On the whole, it is worth to note that the observed complicated internal structure of the fronts, which might comprise several frontal features with enhanced SST gradients, implies that they should be seen as "frontal zones" rather than "fronts" (Fedorov, 1986; Rodionov and Kostianoy, 1998; Kostianoy and Lutjeharms, 1999).

Satellite data showed that the close approach and transient interaction of the AF, SSTF, and SAF can occur not only in the Crozet and Kerguelen basins, but at 20–30°E as well. Moreover, the formation of the northward meander of the AF in the Kerguelen Basin results in the increase of the distance between the AF and the SSTF/SAF. It should be pointed out that both the present satellite data set with a spatial resolution of 18 km and hydrographic surveys with a resolution around 1–2 km might be inadequate for an accurate analysis of the merged fronts in the Crozet Basin whose main goal is to distinguish individual fronts among this complex structure.

The analysis of SST of the fronts have pointed out the decoupling between frontal position and SST of the fronts so that it appears hazardous to determine frontal positions in terms of strictly defined temperature ranges.

The SST ranges inferred from satellite data (1997–1999) for each front are broader than those previously reported in the literature. This discrepancy between the SST ranges based on in situ measurements and satellite data can be explained by the interannual and seasonal variability of SST, the larger spatial and temporal coverage of satellite data, the north–south displacements of the fronts, and finally by the different methods for the determination of SST ranges. On the other hand, satellite-derived SST ranges can be slightly overestimated because of the possible errors in the identification of a front when two or more fronts are closely spaced. Synchronous satellite and field observations could resolve these discrepancies.

Acknowledgements

This research was supported by the Belgian Federal Office for Scientific, Technical and Cultural Affairs (SSTC) through the Belgian Scientific Program on the Antarctic (contract A4/DD/B14 and EV/7/12E). The work was performed mostly at the Chemical Oceanography Unit and GeoHydrodynamics and Environment Research (GHER) of the Liege University where A.G.K. held the Belgian SSTC Research Fellowship in 2000 and 2002. This opportunity and the hospitality of the Chemical Oceanography Unit and GHER are greatly appreciated. The support by the SSTC is gratefully acknowledged. This is MARE contribution no. 31. The authors would like to thank anonymous reviewers for comments and suggestions that much improved the original manuscript.

References

Belkin, I.M., 1989a. Alteration of the front distributions in the Southern Ocean near the Crozet Plateau. Dokl. USSR Acad. Sci., Earth Sci. Sect. 308, 265–268 (English translation).

Belkin, I.M., 1989b. Thermohaline structure, hydrological fronts, and flux of the Antarctic Circumpolar Current in the central part of the Indian sector of the Southern Ocean. Antarktika 28, 97–112 (in Russian).

Belkin, I.M., Gordon, A.L., 1996. Southern Ocean fronts from the Greenwich meridian to Tasmania. J. Geophys. Res. 101 (C2), 3675–3696.

Colton, M.T., Chase, R.R.P., 1983. Interaction of the Antarctic Circumpolar Current with bottom topography: an investigation using satellite altimetry. J. Geophys. Res. 88 (C3), 1825–1843.

Deacon, G.E.R., 1982. Physical and biological zonation in the Southern Ocean. Deep-Sea Res. 29 (1), 1–15.

Deacon, G.E.R., 1983. Kerguelen, Antarctic and subantarctic. Deep-Sea Res. 30 (1), 77–81.

Dehairs, F., Lancelot, C., André, L., Frankignoulle, M., Deleersnijder, E., Cattaldo, T., Elskens, M., Kopczynska, E.E., Becquevort, S., Schoemann, V., Hannon, E., Fagel, N., Cardinal, D., Navez, J., Delille, B., Kostianoy, A.G., 2001. An integrated

approach to assess carbon dynamics in the Southern Ocean, Final Report. Office for Scientific, Technical, and Cultural Affairs, Belgium.

Djenidi, S., Kostianoy, A.G., Sheremet, N.A., Elmoussaoui, A., 2000. Seasonal and interannual SST variability of the North-East Atlantic Ocean. Oceanic Fronts and Related Phenomena (Konstantin Fedorov International Memorial Symposium), IOC Workshop Report Series, No. 159. UNESCO, GEOS, Moscow, 99–105.

Edwards, R.J., Emery, W.J., 1982. Australasian Southern Ocean frontal structure during summer 1976–77. Aust. J. Mar. Freshw. Res. 33, 3–22.

Fedorov, K.N., 1986. The Physical Nature and Structure of Oceanic Fronts. Springer-Verlag, Berlin. 333 pp.

Fedorov, K.N., Ginsburg, A.I., 1992. The Near-Surface Layer of the Ocean. Utrecht, The Netherlands. 259 pp.

Gambéroni, L., Géronimi, J., Jeanin, P.F., Murail, J.F., 1982. Study of frontal zones in the Crozet–Kerguelen region. Oceanol. Acta 5 (3), 289–299.

Griffiths, R.W., Pearce, A.F., 1985. Instability and eddy pairs on the Leeuwin Current south of Australia. Deep-Sea Res. 32 (12), 1511–1534.

Grundlingh, M.L., 1978. Drift of a satellite-tracked buoy in the southern Agulhas Current and Agulhas Return Current. Deep-Sea Res. 25 (12), 1209–1224.

Holliday, N.P., Read, J.F., 1998. Surface oceanic fronts between Africa and Antarctica. Deep-Sea Res. 45 (2–3), 217–238.

Kazmin, A.S., Rienecker, M.M., 1996. Variability and frontogenesis in the large-scale oceanic frontal zones. J. Geophys. Res. 101 (C1), 907–921.

Kort, V.G., 1981. Mesoscale variability of currents and temperature in the Southern Ocean from drifting buoys data. Oceanology 21 (3), 291–298 (English translation).

Kostianoy, A.G., Lutjeharms, J.R.E., 1999. Atmospheric effects in the Angola–Benguela frontal zone. J. Geophys. Res. 104 (C9), 20963–20970.

Legeckis, R., Cresswell, G., 1981. Satellite observations of sea-surface temperature fronts off the coast of western and southern Australia. Deep-Sea Res. 28 (3A), 297–306.

Lutjeharms, J.R.E., 1981. Spatial scales and intensities of circulation in the ocean areas adjacent to South Africa. Deep-Sea Res. 28 (11A), 1289–1302.

Lutjeharms, J.R.E., Roberts, H.R., 1988. The Natal Pulse: an extreme transient on the Agulhas Current. J. Geophys. Res. 93 (C1), 631–645.

Lutjeharms, J.R.E., Valentine, H.R., 1984. Southern Ocean thermal fronts south of Africa. Deep-Sea Res. 31 (12), 1461–1475.

Lutjeharms, J.R.E., van Ballegooyen, R.C., 1984. Topographic control in the Agulhas Current system. Deep-Sea Res. 31 (11), 1321–1337.

Lutjeharms, J.R.E., van Ballegooyen, R.C., 1988. The retroflection of the Agulhas Current. J. Phys. Oceanogr. 18 (11), 1570–1583.

Moore, J.K., Abbott, M.R., Richman, J.G., 1997. Variability in the location of the Antarctic Polar Front (90°–20°W) from satellite sea surface temperature data. J. Geophys. Res. 102 (C13), 27825–27833.

Moore, J.K., Abbott, M.R., Richman, J.G., 1999. Location and dynamics of the Antarctic Polar Front from satellite sea surface temperature data. J. Geophys. Res. 104 (C2), 3059–3073.

Neiman, V.G., Burkov, V.A., Scherbinin, A.D., 1997. Dynamics of the Indian Ocean. Scientific World, Moscow. 231 pp., in Russian.

Orsi, A.H., Whitworth III, T., Nowlin Jr., W.D. 1995. On the meridional extent and fronts of the Antarctic Circumpolar Current. Deep-Sea Res. 42 (5), 641–673.

Pakhomov, E.A., Froneman, P.W., Ansorge, I.J., Lutjeharms, J.R.E., 2000. Temporal variability in the physico-biological environment of the Prince Edward Islands (Southern Ocean). J. Mar. Sys. 26 (1), 75–95.

Park, Y.H., Gambéroni, L., 1995. Large-scale circulation and its variability in the south Indian Ocean from TOPEX/Poseidon altimetry. J. Geophys. Res. 100 (C12), 24911–24929.

Park, Y.H., Gambéroni, L., 1997. Cross-frontal exchange of Antarctic Intermediate Water and Antarctic Bottom Water in the Crozet Basin. Deep-Sea Res. I 44 (5), 963–986.

Park, Y.H., Gambéroni, L., Charriaud, E., 1991. Frontal structure and transport of the Antarctic Circumpolar Current in the south Indian Ocean sector, 40°–80°E. Mar. Chem. 35, 45–62.

Park, Y.H., Gambéroni, L., Charriaud, E., 1993. Frontal structure, water masses, and circulation in the Crozet Basin. J. Geophys. Res. 98 (C7), 12361–12385.

Park, Y.H., Charriaud, E., Craneguy, P., Kartavtseff, A., 2001. Fronts, transport, and Weddell Gyre at 30°E between Africa and Antarctica. J. Geophys. Res. 106 (C2), 2857–2898.

Pollard, R.T., Read, J.F., 2001. Circulation pathways and transports of the Southern Ocean in the vicinity of the Southwest Indian Ridge. J. Geophys. Res. 106 (C2), 2881–2898.

Read, J.F., Pollard, R.T., 1993. Structure and transport of the Antarctic Circumpolar Current and Agulhas Return Current at 40°E. J. Geophys. Res. 98 (C7), 12281–12295.

Rintoul, S.R., Bullister, J.L., 1999. A late winter hydrographic section from Tasmania to Antarctica. Deep-Sea Res. I 46 (8), 1417–1454.

Rintoul, S.R., Sokolov, S., 2001. Baroclinic transport variability of the Antarctic Circumpolar Current south of Australia (WOCE repeat section SR3). J. Geophys. Res. 106 (C2), 2815–2832.

Rintoul, S., Trull, T.W., 2001. Seasonal evolution of the mixed layer in the Subantarctic Zone south of Australia. J. Geophys. Res. 106 (C12), 31447–31462.

Rintoul, S.R., Donguy, J.R., Roemmich, D.H., 1997. Seasonal evolution of upper thermal structure between Tasmania and Antarctica. Deep-Sea Res. I 44 (7), 1185–1202.

Rodionov, V.B., Kostianoy, A.G., 1998. Oceanic Fronts in the Seas of the North European Basin. GEOS, Moscow. 293 pp., in Russian.

Sarukhanian, E.I., Smirnov, N.P., 1986. Water Masses and Circulation of the Southern Ocean. Gidrometeoizdat, Leningrad. 288 pp., in Russian.

Smythe-Wright, D., Chapman, P., Duncombe Rae, C., Shannon, L.V., Boswell, S.M., 1998. Characteristics of the South Atlantic subtropical frontal zone between 15°W and 5°E. Deep-Sea Res. I 45 (1), 167–192.

Tomczak, M., Godfrey, J.S., 1994. Regional Oceanography: An Introduction. Pergamon, New York. 422 pp.